A distinctive signature in the Raman and photoluminescence spectra of intercalated PbI_2

2006 J. Phys.: Condens. Matter 18 8899

(http://iopscience.iop.org/0953-8984/18/39/020)

INSTITUTE OF PHYSICS PUBLISHING JOURNAL OF PHYSICS: CONDENSED MATTER

J. Phys.: Condens. Matter **18** (2006) 8899–8912 doi:10.1088/0953-8984/18/39/020

A distinctive signature in the Raman and photoluminescence spectra of intercalated PbI_2

N Preda[1], L Mihut[1], M Baibarac[1], I Baltog[1] and S Lefrant[2]

[1] National Institute for Physics of Materials, Laboratory of Optics and Spectroscopy, Bucharest, PO Box MG-7, R-77125, Romania
[2] Institut des Materiaux de Nantes, Laboratoire Physique des Materiaux et Nanostructures, 2 rue de la Houssiniere, B.P. 32229, 44322 Nantes, France

E-mail: ibaltog@infim.ro

Received 17 May 2006, in final form 28 July 2006
Published 15 September 2006
Online at stacks.iop.org/JPhysCM/18/8899

Abstract

Through correlated studies using scanning electron microscopy (SEM), Raman spectroscopy and low-temperature photoluminescence (PL) we have demonstrated that the intercalated PbI_2 with ammonia, poly (vinyl alcohol) and polyacrylamide are characterized by a distinctive signature in the Raman and photoluminescence spectra. After intercalation, the Raman spectrum of PbI_2 reveals an orthorhombic structure, identical with that observed on the micrometric scale, of $KPbI_3$ rod-like particles resulting from the reaction between $Pb(NO_3)_2$ and KI, carried out in liquid media such as ethanol and acetonitrile. The rods and the intercalated PbI_2 are characterized by a new and strong emission band at 2.23 eV (about 550 nm) that appears at 77 K under an excitation wavelength of about 340 nm. Modification of the Raman and PL spectra results from a compressing effect produced by the penetration between the PbI_2 layers of different molecular species. The compression acting primarily on the iodine layers has the result of lowering the contribution of the 5p states of I^- ions to the constitution of the electronic level situated at the top of valence band of PbI_2, so that the photoluminescence of intercalated PbI_2 acquires the characteristics of Pb^{2+} emission when it is dissolved in an alkali halide crystal.

1. Introduction

In recent times, the family of solids in which the atoms are arranged in layers with strong internal chemical bonds and weak van der Waals forces that keep the layers together has attracted much interest for fundamental research and technological applications. This is motivated by the ability to model new properties resulting from the intercalation between layers of foreign atoms, ions and molecules. The macroscopic physical properties of these materials are strongly anisotropic. Graphite is probably the most familiar of such layered materials (LM), but there are also many sulfides (and other chalcogenides), halogenides and silicates (e.g. mica), which adopt layer structures. In general, the single crystals of LM are easily cleaved into thin

flakes due to the weak bonding between the layers. Among the most important applications of layered structure materials may be mentioned those of lubrication, high catalytic activity, use as electrodes in electrochemical photocells for solar energy conversion, active materials in the rechargeable batteries etc.

Intercalation, the insertion of guest atomic and molecular entities into the architecture of a crystal, is an efficient route for generating new materials with novel properties [1, 2]. It requires, on the one hand, a host structure in which atoms form a strong binding network that remains unchanged on intercalation and, on the other, the existence of vacant sites of suitable sizes which permit the diffusion of the guest species into the host structure. Intercalation produces an increase in the *c*-axis parameter. As a general rule, an intercalated structure exhibits an increased degree of disorder, an alternation of intercalated and non-intercalated regions.

Lead iodide is an LM material that easily satisfies the requirements to accommodate very large guest molecules in the interlayer space by the free adjustment of the interlayer separations [3–9]. Lead iodide, as a direct band gap semiconductor of about 2.5 eV, is characterized by a spatial repetition of three planes, I–Pb–I. In the bulk form, the PbI_2 crystal features a strong intralayer chemical bonding and a weak interlayer bonding involving van der Waals interactions [10]. As in any layered single crystal, PbI_2 is strongly anisotropic; under band-to-band light irradiation the PbI_2 crystal is a good photoconductor along the layers, but less so across them. Such materials, often referred to as 'bi-dimensional materials', have properties connected to the nanometre-scale thickness of the layers. The strong excitonic emission, of super-radiant type, observed ordinarily in PbI_2 as well as in other halogenides with layered structures such as BiI_3, CdI_2, etc could be considered a quantum confinement effect relieved by the exciton's condensation in layers of nanometre thicknesses [11–17].

For the PbI_2 crystal, theoretical calculations supported by optical absorption, PL and ellipsometric measurements established that the uppermost valence band is dominated by the 6s state of Pb^{2+} ion with some 5p iodine admixture. The lowest energy of the conduction band is composed mainly of the 6p lead atomic orbital [8, 18, 19]. This explains the cationic nature of the strong excitonic luminescence that appears under band-to-band light excitation. On intercalation, interlayer penetration of foreign molecules takes place which, by compression, contribute to the destruction of the two-dimensional connectivity of the original lamellar structure.

The final effect consists of the modification of the uppermost valence band, i.e. in a reduction of the contribution of the 5p states of I^- ions. This induces a weakness in the interaction between the lead ion and iodine electron within a layer, so that the direct and backward transition $^1S_0 \rightarrow {}^3P_1$ of the Pb^{2+} ions shifts towards higher energies, acquiring the feature of an intra-ion transition. A shift of the cationic absorption band to higher energies was indeed observed in PbI_2 intercalated with a variety of Lewis base ligands, including hydrazine [3], pyridine [4], aniline [5, 6] and ammonia [7]. In photoluminescence, a similar effect becomes observable through new emission bands up-shifted with different decay characteristics from those recorded in non-intercalated PbI_2 crystals.

Another effect of the intercalation can be observed in the change in the phonon spectrum, which may be understood qualitatively in terms of a simple crystal field model. The lead coordination geometry in the PbI_2 single crystal is that of a trigonal antiprism (D_{3d}). After reaction with a guest molecule, for example pyridine (py), the $PbI_2(py)_2$ complex is formed in which the D_{3d} coordination geometry is reduced to orthorhombic and the lead atom is six coordinated by two ligand nitrogen atoms and four iodides, bridged pair-wise to neighbouring lead atoms. X-ray diffraction studies on intercalated PbI_2 evidence that a one-dimensional structure along the *c*-axis is formed [4, 6–9]. Such a new structure displays a different phonon spectrum to that observed in both infrared and Raman spectroscopy of PbI_2 intercalated with

ammonia, methylamine, ethylamine and butylamine [6]. The Raman spectrum of ammonia intercalated PbI_2 is complex and entirely different from that of the pristine material. It reveals an orthorhombic structure characterized by the appearance of a number of sharp low-frequency Raman lines below 100 cm^{-1}. A surprising result is that the Raman spectrum of the aggregates of PbI_2 obtained from a colloidal suspension in acetonitrile (ACN) [20] is similar to the Raman spectra of ammonia or pyridine intercalated PbI_2 [4, 7] in all these cases revealing an orthorhombic structure.

Thus, in the light of the above observations, we state that the goal of this paper is to demonstrate that the PbI_2 samples intercalated with different guest species (ammonia, polyacrylamide and poly(vinyl alcohol)) are characterized by the same Raman and luminescence spectra as those recorded on micrometre-size rod-like particles resulting from the reaction between $Pb(NO_3)_2$ and KI, carried out in excess KI.

2. Experimental details

Practically, the intercalation can be achieved in three ways: adding the guest species during LM synthesis; diffusion from vapour or liquid phase into the LM samples; or electrochemically via placing an LM cathode into an electrolyte containing ions of the guest species.

In this work, three types of intercalated PbI_2 samples were prepared: (i) by the diffusion of ammonia vapours into micrometric crystalline powder obtained by mechanical crumbling of a PbI_2 single crystal grown from the melt; (ii) by the chemical reaction between an aqueous solution of lead nitrate (5 cm^3; 0.01 M) and aqueous solution of potassium iodide (5 cm^3; 0.05 M) carried out under vigorously ultrasonic homogenizing in aqueous polyacrylamide solution (100 cm^3; 0.01%); and (iii) by slowly cooling to room temperature over a few hours a boiling saturated aqueous PbI_2 solution to which was added, prior to cooling, aqueous solutions of poly vinyl alcohol or polyacrylamide (0.01%). The rods resulting from the chemical reaction of KI with $Pb(NO_3)_2$ carried out in ACN according to the procedure described in [21], considered as the prototype of intercalated PbI_2, were used for comparison. During the synthesis, the sudden appearance of a yellow colour is evidence for the formation of colloidal particles dispersed in the synthesis medium; these sediment slowly to form a deposit on the bottom of the vessel.

The Raman spectra were recorded under 676.4 nm excitation light at room temperature in backscattering geometry with a Jobin Yvon T64000 spectrometer equipped with a microprobe (objective magnification power, 100×; numerical aperture, 0.95) allowing the laser spot to be focused on the sample within a micrometre scale. This facility has permitted Raman inspection of individual particles of different sizes and shapes.

The PL spectra at liquid nitrogen temperature (LNT) were recorded in reflection at right-angle geometry under continuous excitation at $\lambda_{exc} = 457.9$ nm using a Coherent Innova 90 argon ion laser. For excitation at 340 nm, a high-pressure Hg lamp (500 W) fitted with a monochromator was used. The spectral analysis system was a SPEX double monochromator, equipped with a cooled EMI photomultiplier and a photon counting system.

A pulsed nitrogen laser ($\lambda_{emis} = 337.1$ nm) with 5 ns pulse duration was used as excitation source for the measurement of decay time. Recording of the luminescence decay was performed using a fast photomultiplier EMI 9818 B and a Tektronics TDS 320 two-channel oscilloscope interfaced with a computer.

3. Results and discussion

Recently, we have shown by SEM images that the reaction between $Pb(NO_3)_2$ and KI, carried out in different liquid media such as water, methanol, ethanol (EtOH) and ACN, results in

platelets and rod-like particles of micrometric and nanometric size. Generally, both particles are formed [21]. Raman and PL spectroscopic studies demonstrated that the platelets are PbI_2 particles.

When EtOH is used as the reaction medium, both platelets and rods are formed from the beginning of the reaction. By storing the synthesis solution, an increase in the particle size similar to that in a crystalline growth process can be observed. Thus, in accordance with these observations, the generation of rod-like particles in EtOH can be explained by the reaction

$$2Pb(NO_3)_2 + 5KI \rightarrow PbI_2 + KPbI_3 + 4KNO_3. \quad (1)$$

This suggests that the appearance of PbI_2 platelets and rods from the beginning of the reaction is associated with the $KPbI_3$ mixed compound. This conclusion concerning the chemical constituency of the rod-like particles is supported by the striking resemblance of the low-temperature Raman spectrum recorded on an isolated rod with that of a $CsPbCl_3$ crystal in the orthorhombic structure present at low temperature [21, 22].

A remarkable effect can be observed when ACN is used as the buffer liquid [21]. The rods' formation is foregone by the appearance of small hexagonal platelets whose Raman spectrum is identical to that of the lead iodide crystal itself. These platelets, deposited on the bottom of the preparation vessel, transform slowly into thin rods, forming expanded tufts. In this case, the formation of rod-like particles could be described by two consecutive reactions: the first one in which primarily PbI_2 platelets are formed, followed by the second one in which the platelets transform into rods. Taking into account that these reaction take place in an excess of KI, it seems quite reasonable to suppose that the rods have the same chemical composition as those formed in EtOH:

$$Pb(NO_3)_2 + 2KI \rightarrow PbI_2 + 2KNO_3 \quad (2)$$

$$PbI_2 + KI \rightarrow KPbI_3. \quad (3)$$

We now turn to the experimental data.

SEM yielded irrefutable evidence that the synthesis procedures mentioned above result in platelets and rods. Figures 1(a) and (b) show that the reaction between $Pb(NO_3)_2$ and KI carried out in EtOH and ACN results in either platelets and rods or only rods, respectively. Observing the morphological aspect, it can be seen that the rods produced in EtOH and ACN are different: the insets of figure 1 show that the rods appear in the former case as rectangular prisms with clear edges and clean faces, while in the latter case they are approximately cylindrical prisms with roughened surfaces. These details may indicate some differences in their manner of formation that will be considered below.

Figures 1(c) and (d) show pictures of the particles formed when a boiling saturated aqueous PbI_2 solution containing 0.01% poly (vinyl alcohol) and polyacrylamide, respectively, was cooled slowly to room temperature. The same two types of particles were observed; the proportion of each one, however, depended on the specific conditions of synthesis. Comparing platelets formed in the presence of poly (vinyl alcohol) or polyacrylamide, figures 1(c) and (d) respectively, with those resulting from the reaction between $Pb(NO_3)_2$ and KI carried out in EtOH, figure 1(a), one observes that these appear as thin lamellar structures and large area in the former case and hexagonal prismatic close-packed structures in the latter case.

These different morphological aspects are better illustrated in figure 2, where the platelets formed by the reaction (1) carried out in water (figure 2(a)), in 0.01% polyacrylamide aqueous solution (figure 2(b)) and in water mixed with ACN 1:1 v/v (figure 2(c)) are presented.

The Raman spectra recorded for individual particles gives a convincing proof that the platelets and rods belong to different compounds. The platelets display the well-known Raman

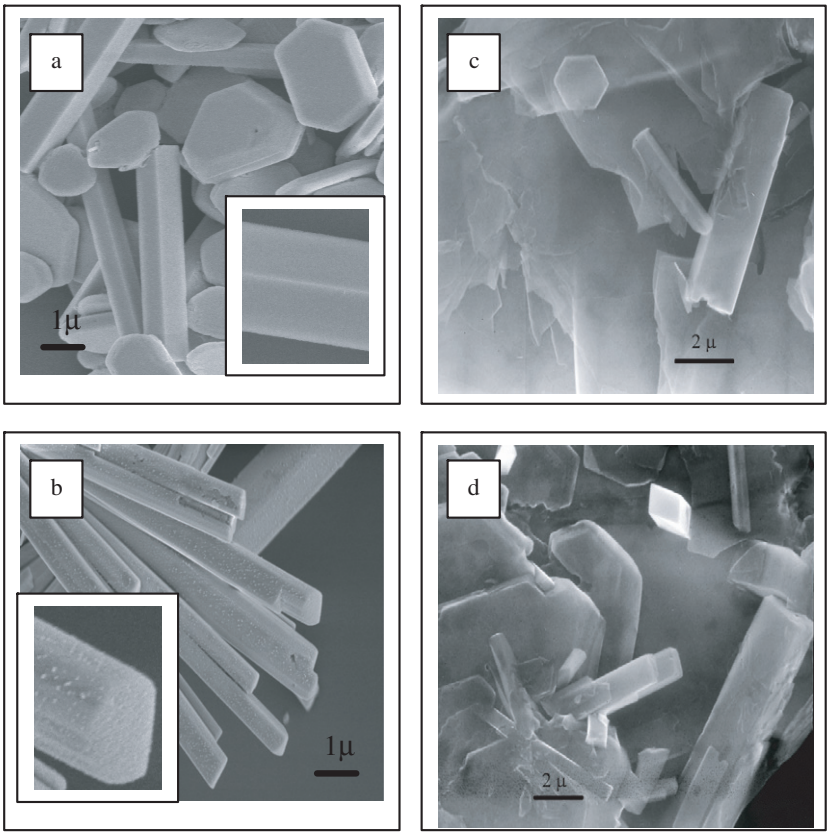

Figure 1. SEM images of the particles produced by chemical reaction between $Pb(NO_3)_2$ and KI carried out in ethanol (a) and acetonitrile (b) or by cooling a boiling saturated aqueous PbI_2 solution containing 0.01% poly (vinyl alcohol) (c) or polyacrylamide (d) to room temperature.

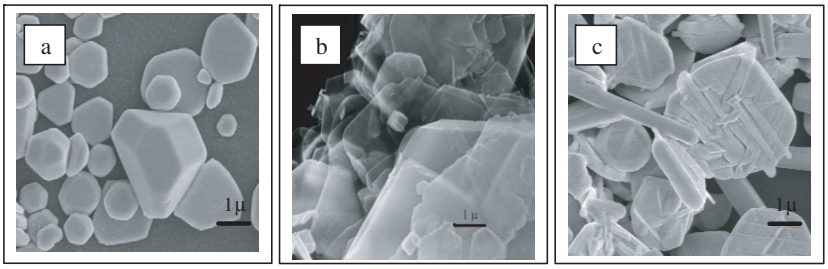

Figure 2. SEM images of the particles produced in the reaction between $Pb(NO_3)_2$ and KI carried out (a) in water, (b) water containing 0.01% polyacrylamide and (c) water acetonitrile mixture (1:1 v/v).

spectrum of the PbI_2 (figure 3(a)), the same as in the case when the measurement was performed on a PbI_2 crystalline sample cleaved from a melt-grown crystal [23].

Figures 3(b)–(d) show the Raman spectra of rods measured on samples prepared by different routes, i.e. by the reaction between $Pb(NO_3)_2$ and KI carried out in ACN, by the slow cooling to room temperature of a boiling saturated aqueous PbI_2 solution containing 0.01% polyacrylamide, and by the diffusion of ammonia vapour into micrometric crystalline PbI_2

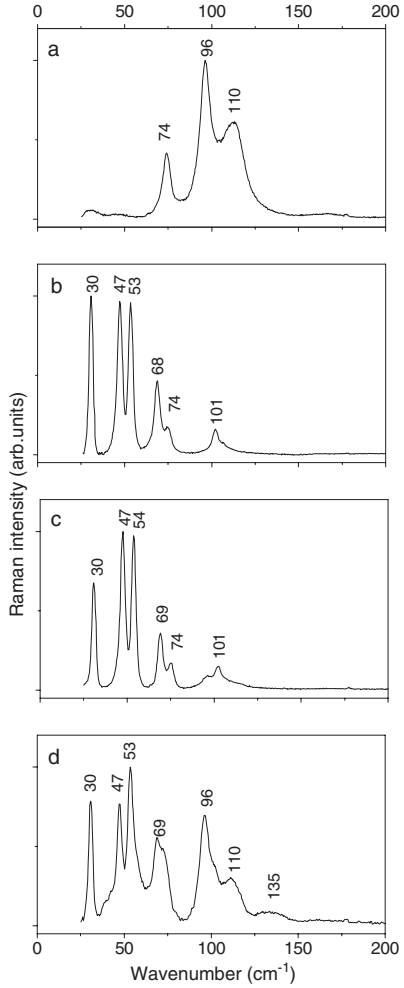

Figure 3. Raman spectra at $\lambda_{exc} = 676.4$ nm of: (a) PbI_2 platelets; (b) rods resulting from the reaction between $Pb(NO_3)_2$ and KI carried out in acetonitrile; (c) rods produced by slowly cooling a boiling saturated aqueous PbI_2 solution containing 0.01% polyacrylamide to room temperature; (d) ammonia intercalated PbI_2 sample prepared by diffusion of ammonia into micrometric crystalline PbI_2 powder.

powder, respectively. The same Raman spectrum associated with the rods was recorded for the sample prepared from the cooling of a boiling saturated aqueous PbI_2 solution containing 0.01% poly (vinyl alcohol). We notice that the Raman spectra of all rod-like particles, regardless of the synthesis routes used in their preparation, are strongly dependent on the direction of observation and excitation relative to the principal axes of the particle, and disclose an orthorhombic crystalline system.

In the PbI_2 crystal, the weak interlayer forces make possible a different stacking of layers, which results in a polytypic structure. Several polytypes (2H, 4H, 6H, 8H, 10H, 14H, 22H, 26H, 12R, and 18R, where H and R indicates hexagonal and rhombohedral polytypes, respectively) were reported [24]. The most frequently observed are 2H and 4H polytypes. The unit cell of the 2H-polytype contains only one layer packet, whereas in 4H polytype it embraces two layers. In general, the as-grown PbI_2 crystals contain 2H polytypes and at 425K undergo an irreversible 2H $\rightarrow$ 4H inter-polytype transition [25]. On increasing the temperature of thermal treatment, the 2H polytypes transform into polytypes of high order whose unit cells increase along the *c*-axis, which in the Raman spectrum is indicated by the appearance of new lines. The 2H and 4H polytypic structures belonging to the space group D^3_{3d} and C^4_{6v}, respectively,

are the most frequently observed. Classified according to the irreducible representation, the normal vibration modes of 2H and 4H polytypes are $A_{1g} + E_g + 2A_u + 2E_u$ and $3A_1 + 3B_1 + 3E_1 + 3E_2$, respectively [25]. Two prominent Raman bands at about 74 and 96 cm^{-1} are displayed for 2H and 4H polytypes, which are associated with the vibration modes (E_g, A_{1g}) and (E_2^1, A_1^1), respectively. Besides, depending on the origin of the PbI_2 sample, often additional Raman bands at 15, 30, 51, 78, 110 cm^{-1} are observed [23]. PbI_2 samples, cleaved from a crystal ingot grown from the melt by the Bridgman method, show a systematic increase in the relative intensity of the band at 30 cm^{-1} when submitted to an inter-polytype irreversible transformation from 2H into 4H [23, 26] by thermal annealing at about 425 K. At first sight, the simultaneous appearance of the bands located at 15 and 30 cm^{-1}, at both 676.4 and 514.5 nm excitation wavelengths, suggests that these are interconnected as a single phonon line and two phonon lines, respectively. Another explanation, deduced from the neutron scattering studies, associates the Raman band at 30 cm^{-1} to a longitudinal acoustic (LA) phonon describing a compressive rigid-layer mode [25]. The latter explanation is very well supported by the theoretical calculations of the force constants that describe the crystal vibrations along the *c*-axis [26]. In this frame, the Raman line at 30 cm^{-1} is associated with an interlayer compressional force constant of about 7 N m^{-1} [26]. Although the LA phonon related to the rigid-layer mode is Raman inactive, the appearance and enhancement of the Raman band at 30 cm^{-1} observed systematically in the Ag-doped PbI_2 crystals indicates that, through the insertion of foreign atoms into PbI_2 crystal structure, this vibration mode becomes Raman active. Returning to figures 3(b)–(d), we associate the strong Raman band at 30 cm^{-1} with an LA phonon, activated as result of the compression produced by the intercalation of different molecular species between the PbI_2 layers.

Similar to the Raman spectrum of $CsPbCl_3$ in a *Pnma* orthorhombic structure [22], the figures 3(b)–(d) reveal, in the low-frequency range, two sets of doublets situated at about (47, 54) cm^{-1} and (68, 74) cm^{-1} that are associated with the transverse optical (TO) phonons. These doublets, originating in the vibration modes (E_1^2, E_2^2) and (E_2^1, E_1^1) of the 4H-PbI_2 polytype, together with the strong Raman band at about 30 cm^{-1}, appear as the main Raman signature for the intercalated PbI_2 samples. Depending on the degree of intercalation, the original modes of PbI_2 almost vanish.

The uniqueness of the Raman spectra for the rods-like particles produced in EtOH and ACN is somewhat surprising, taking into account the SEM images, figures 1(a) and (b), which reveal some differences. The primary question that arises is whether the rods indicated in the reactions (1) and (3) by the chemical formula $KPbI_3$ are really the same. The morphological aspect of the rods produced in EtOH, and the fact that their size increases if the synthesis solution is stored over a longer time (akin to a growing crystal process), can be arguments that these particles are micrometric single crystals resembling the compound $CsPbCl_3$, which has an orthorhombic structure at low temperature [22].

For the rods produced in ACN, because these start to grow from platelet-like particles, one can consider another formation mechanism that consists of the diffusion of potassium and iodine ions between iodine layers of the PbI_2 lattice. A similar kind of diffusion of ACN molecules between iodine layers of PbI_2 lattice might also occur. In this way, an intercalated structure, belonging to an orthorhombic crystalline system, is formed. Actually, this transformation into an intercalated structure may be inferred by rewriting the $KPbI_3$ from the reaction (3) as PbI_2(KI), where KI plays the role of guest species. In this scenario, the rods can be either uniform intercalated structures or structures in which the non-intercalated PbI_2 micro-zones alternate with PbI_2 micro-zones inserted with guest entities.

Returning to figure 3, one must underline that the Raman spectra are able to reveal platelets and rods separately, but are not able to specify whether the rods represent a

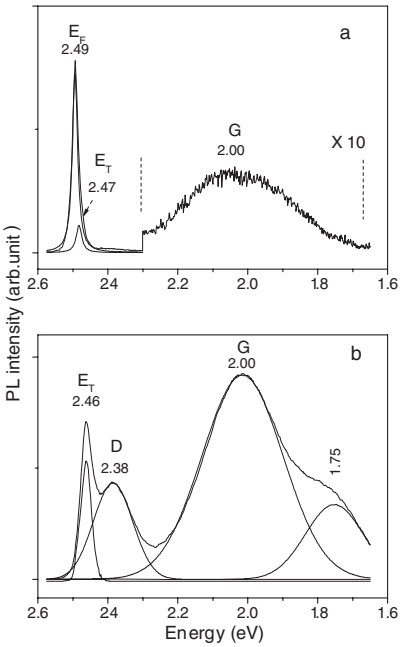

Figure 4. Photoluminescence at liquid nitrogen temperature of PbI_2 samples extracted from a Bridgmann-grown PbI_2 single crystal: (a) cleaved crystalline slide; (b) micrometric crystalline powder obtained by mechanical crumbling. $\lambda_{exc} = 457.9$ nm.

$KPbI_3$ crystalline structure or an intercalated PbI_2 compound also displaying an orthorhombic structure. This uncertainty can be eliminated through the analysis of decay times and the study of photoluminescence spectra at 77 K obtained under different excitation wavelengths.

If the rods are really $KPbI_3$-type particles, then they should, in the same way as the $CsPbCl_3$ crystal in the orthorhombic phase, present a luminescence spectrum displaying a strong emission band characterized by a decay time in the nanosecond range originating from an excitonic recombination.

The PL of the two types of particles resulting from the reaction between $Pb(NO_3)_2$ and KI, i.e. platelets and rods, discloses a distinctive feature. As excitation light approaches or surpasses the fundamental absorption band, 488 or 457.9 nm, the platelets exhibit a PL spectrum consisting of two intense bands, labelled E and G, centred around 2.5 and 2.0 eV, respectively, similar to those observed from a crystalline sample cleaved from a PbI_2 single-crystal grown from the melt [21].

The detailed PL studies of platelets and rods need to be set against the emission spectra of two types of PbI_2 samples retrieved from a Bridgman-grown PbI_2 single crystal: one as a cleaved crystalline slide (figure 4(a)) and the other one as a micrometric crystalline powder obtained by mechanical crumbling (figure 4(b)). The measurements were made at 77 K under 457.9 nm laser excitation, which corresponds to a band-to-band transition.

As might be expected, the main signature in the PL spectra is given by the excitonic emission, which is an intense E_F band at 2.49 eV originating from the recombination of the free excitons created by the band-to-band irradiation (figure 4(a)). Depending on the sample quality, even in nominally pure crystals, the E_F band presents a small asymmetry on the low-energy side, which discloses a weak band, E_T, down-shifted at about 2.47 eV. This is due to the recombination of the trapped excitons in the imperfections of the crystal lattice [27, 28]. Another component of the PL spectrum is a wide G band at about 2.0 eV, interpreted as originating from a radiative electron–hole recombination process, associated with the presence of the Pb^+ ions created under band-to-band irradiation [21]. The disappearance of the G band

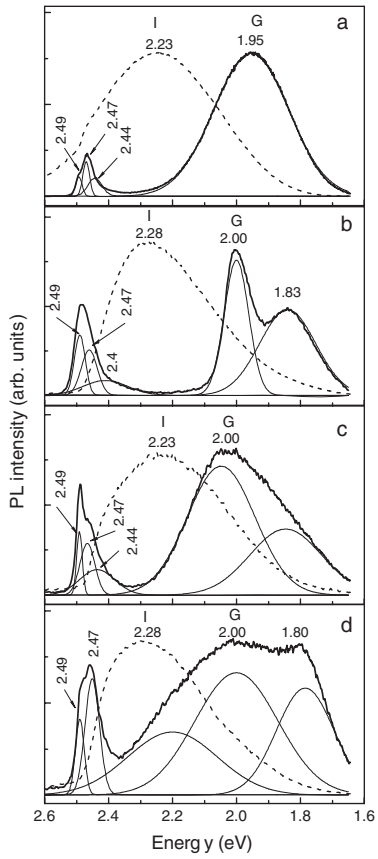

Figure 5. Photoluminescence at liquid nitrogen temperature at $\lambda_{exc} = 457.9$ nm (solid line) and $\lambda_{exc} = 340$ nm (dashed line) of particles resulting from the reaction between $Pb(NO_3)_2$ and KI carried out in acetonitrile (a), ammonia intercalated micrometric crystalline PbI_2 powder (b), particles produced by slowly cooling a boiling saturated aqueous solution of PbI_2 containing 0.01% polyacrilamide to room temperature (c); and particles produced by the reaction between $Pb(NO_3)_2$ and KI carried out in water containing 0.01% polyacrylamide (d).

through the simple removal of the top layer of the sample indicates that it is generated in a thin layer at the crystal surface. The role of surface defects in the generation of the G band is illustrated in figure 4(b). For a PbI_2 crystalline powder, characterized by an increased density of surface defects, the PL spectrum reveals a down-shifted excitonic band arising from the recombination of trapped excitons and an intense G band as its most distinctive detail. Similarly, associated strongly with the presence of Pb^+ ions usually produced near dislocations and cleavage defects, is the D band, whose presence was signaled in both pure and doped crystals [27, 28].

Recently, the G band was reported as a distinct signature in the emission spectrum of the PbI_2 nanometre-sized particles [29, 30]. Its disappearance through annealing and thermal treatment in an iodine atmosphere is an argument for its association with the lattice stoichiometric defects [20].

Except for some variations in intensity, the E, D and G emission bands shown in figure 4 are always present in the PL spectrum of any sample, whether as a crystalline slide or as a crystalline powder prepared from melt crystal growth. Besides, the PL spectrum is preserved, without the appearance of other bands, if the energy of the excitation light is tuned from the edge of the fundamental absorption band towards higher values. This finding is no longer relevant in the case of rod-like particles resulting from the reaction between $Pb(NO_3)_2$ and KI or $Pb(NO_3)_2$ and NaI carried out in different liquids, as well as in the case of the intercalated PbI_2 samples with ammonia, poly (vinyl alcohol) or polyacrylamide. In these cases, figure 5

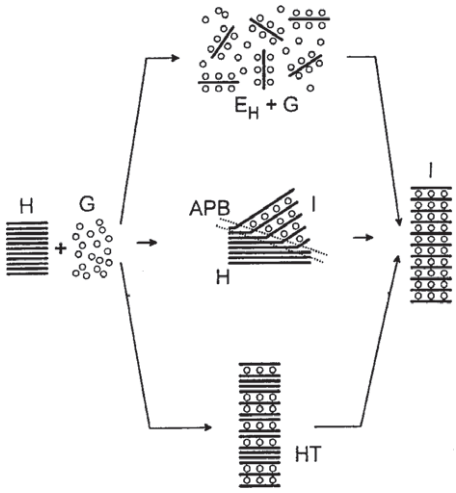

Figure 6. Schematic representation of the intercalation mechanisms: H—host; G—guest; I—intercalate; E_H—exfoliated host layer; APB—advancing phase boundary; and HT—Hendricks–Teller disordered layer structure.

reveals a new band, labelled I (intercalation acronym) at 77 K when the excitation light is about 340 nm. Observing figure 5, the question immediately arises of why, in this figure, the same samples display both types of PL spectra: one associated with the platelets or non-intercalated PbI_2 crystalline powder that are efficiently excited at 457.9 nm, and another excited at 340 nm that contains only the I band as the typical signature of rod-like particles.

An initial answer concerns our inability to perform simultaneous PL measurements on isolated particles, i.e. platelets and rods of micrometric size. This can be a real inconvenience as, from the preparation, powder samples regularly result that contain either platelets and rods or intercalated and non-intercalated PbI_2 particles. However, this explanation cannot be entirely accepted, since we know that, from the reaction between $Pb(NO_3)_2$ and KI carried out in ACN, only rods result. In this case, one must look for another explanation that can be associated with the non-uniformity of the structures, i.e. with the alternation of intercalated and non-intercalated zones in the same particle.

Such a presumption is supported by referring to the SEM images in figure 2. These show particles of different shapes and sizes resulting from the reaction between $Pb(NO_3)_2$ and KI carried out in water, in 0.01% aqueous polyacrylamide, and in water:ACN (1:1 v/v). In the first case, one observes particles of polyhedral form which have grown equally in the hexagonal plane and in the perpendicular direction on the layer. These particles display the well-known Raman and PL spectra of the PbI_2 crystalline particles, shown in figures 3(a) and 4(b), respectively. In the second case, thin hexagonal crystalline layers of large area are observed. These particles, except for two incipient bands arising at about 30 and 50 cm^{-1}, display a Raman spectrum similar to that of the PbI_2 crystalline sample (figure 3(a)) and a PL spectrum that, under excitation at 340 nm (3.646 eV), reveals the I emission band which, in the context of this paper, is considered as being characteristic of an intercalated PbI_2 structure (figure 5(d)). A unique moment in the creation of platelets and rods is displayed in figure 2(c), in which one observes the rods growing from hexagonal platelet structures. The Raman spectrum of such a complex particle appears as a sum spectrum displaying both the lines associated with the platelets and rods. As is expected, the PL spectrum is similar to those presented in figure 5(d).

These data can be explained on the basis of the schematic representation of the intercalation mechanisms illustrated in figure 6. Between an initial state of the host structure (H) and a final uniform intercalated state (I) with the guest species (G), different intermediate structures can

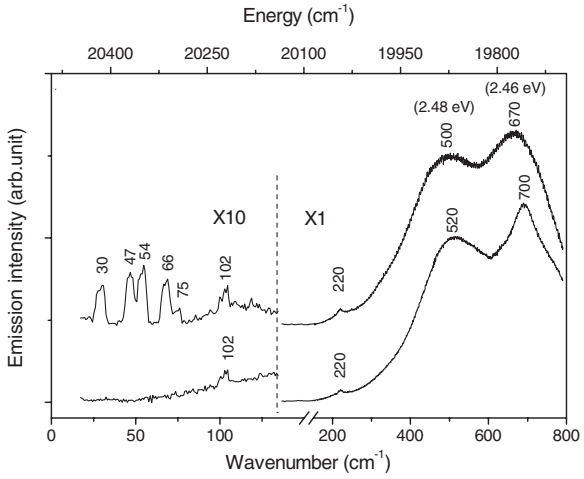

Figure 7. Whole combined emission spectra (Raman and photoluminescence) at 77 K under 488 nm excitation wavelength of platelets (lower curve) and rods (upper curve) resulting from the reaction of $Pb(NO_3)_2$ with KI carried out in 50% water–acetonitrile mixture.

appear as (i) exfoliated host layers (E_H); (ii) an advancing phase boundary (APB) representing an area of the crystal which, immediately at the beginning of the reaction, is replaced by the intercalated form; and (iii) different Hendricks–Teller disordered structures [31]. In this framework, the figures 2(b) and (c) can be readily associated with the exfoliated host layers and advancing phase boundary structures, respectively.

Besides, it has to take into account that an intercalation phase does not fill up the interlayer space uniformly. From the diffusion of guest species between the crystalline layers results galleries that form networks of nanofolds. The whole process is accompanied by a local lattice expansion, which is constrained by the rigid adjacent layers, leading to a build up of three-dimensional strain and stress in the intercalation layer, so that there finally results an alternation of intercalated and non-intercalated micro-zones, even inside a layer.

Using the scheme in figure 6, the $KPbI_3$ rods formed by the reaction (3) in ACN, rewritten as PbI_2(KI), could be viewed as Hendricks–Teller disordered structures in which the intercalated and non-intercalated PbI_2 zones alternate. With such a model, a double signature of platelet and rod in the PL spectra presented in figure 3(a) is not quite unexpected. A convincing demonstration is given in figure 7, which displays the combined emission spectra, i.e. Raman and PL spectra recorded together at 77 K with 488 nm excitation wavelength on an isolated platelet and an isolated rod.

Both particles exhibit two intense emission bands at about 2.48 and 2.46 eV, located in figure 7 as wide bands at 500 and 670 cm^{-1} respectively, that, according to figure 4, must be associated with the excitonic emission from PbI_2 structures when the excitation corresponds to a band-to band transition. For the rods, such an emission spectrum is credible only if one accepts the existence of PbI_2 micro-zones inside the rod. The alternation of PbI_2 structures with the intercalated PbI_2 micro-zones, as well as in the Hendricks–Teller disordered structure, explains the appearance of two Raman signatures in the same scan: (i) one that consists of the lines at 102 and 220 cm^{-1} associated with the PbI_2 platelet structure, regularly observed when the excitation light is tuned toward higher energies than the edge of the fundamental absorption band [23]; (ii) another one associated with the intercalated PbI_2 structure, i.e. the rod that is characterized by a number of Raman lines appearing in the low-frequency domain. As usual, the platelet spectra revealed only the 102 and 220 cm^{-1} bands. Evidently, in this scenario a uniform intercalated structure has to be characterized by a single emission spectrum like that obtained at 340 nm excitation wavelength.

The transition $^1S_0 \rightarrow {}^3P_1$ of the Pb^{2+} remains the main process in the activation of PL emission in the intercalated PbI_2 structure. Due to the compression produced by the penetration of foreign molecular species between iodine layers, the hybridized electronic level situated at the top of the valence band, formed by the contribution of the 6s and 5p states of Pb^{2+} and I^- ions, undergoes a deformation, by which the share of the 5p states of I^- ions is reduced. Finally, the PL process into intercalated PbI_2 acquires all the characteristics of luminescence due to an intra-ion transition. Such PL is clearly observed when the Pb^{2+} ions are dissolved in an alkali halide crystal.

Returning to the rod-like particles produced in ACN, considered as the prototype of KI intercalated PbI_2, written as PbI_2(KI), we found it interesting to perform an analysis of the PL emission in analogy to the luminescence of Pb^{2+} ions contained as impurity in a KI-like lattice. In accordance with the well-known notation of the absorption bands of ns^2 ions in KI, the transitions $^1S_0 \rightarrow 3P_1$ and $^1S_0 \rightarrow {}^1P_1$ are located at 357 and 318 nm, respectively [32, 33]. Regardless of where the excitation takes place, when the Pb^{2+} ions are dispersed into an alkali halide lattice, the PL spectrum displays two emission bands, labelled A_T and A_X, which in NaI and KI crystals are located about 3.03 eV (408 nm) and 2.06 eV (600 nm), respectively. Besides, these emission bands display, as distinctive signatures, very different decay times (the former is about one nanosecond; latter is hundreds of nanoseconds) [32–34]. The positions and intensities of the A_T and A_X bands depend strongly on the dispersion state of the impurity in the host lattice. A complex mechanism of dipole (impurity–cationic vacancy) aggregation, depending on the impurity concentration and the host matrix, leads to the pile-up of impurities around dislocations and grain boundaries. When the impurity reaches a high degree of aggregation, resulting in a precipitation phase of the type PbI::*n*NaI or PbI::*n*KI, the PL spectrum becomes almost a mirror-like image of the excitation spectrum, and the A_T band is replaced by a new one, down-shifted at 2.65 eV (468 nm), which is formed at the expense of the A_X band [33, 34].

It ought to be mentioned that it is probably only a coincidence that the band G observed at 77 K in PL spectra of the PbI_2 crystal almost superposes on the A_x band of Pb^{2+} dissolved in NaI and KI crystals. The G band originates from the radiative recombination of carriers formed by band-to-band irradiation, which is trapped subsequently on the defects of the PbI_2 crystal and in surface defects. Such a luminescence process is, in general, characterized by a short decay time, of the order of a few tens of nanoseconds. The A_x band, resulting from a Pb^{2+} intra-ionic transition, displays a much longer decay time, of the order of hundreds of nanoseconds [33, 34].

The intercalation of foreign species into the PbI_2 crystal results in a compression of the adjacent iodine layers that results in a reduction in the interaction between the lead ion and the iodine electron within a layer. In this way, the forward and backward $^1S_0 \rightarrow {}^3P_1$ transitions of the Pb^{2+} ion occurring in the semiconducting PbI_2 crystal changes, acquiring the characteristics of a Pb^{2+} intra-ion transition. These transitions are well known in the spectra of lead-doped alkali halide crystals.

In this context, we are tempted to regard the I emission band as having the same origin as the A_x band, both displaying a decay time of the order of few microseconds. An argument in this sense is given in figure 8, where one sees that the G and I luminescence bands are characterized by very different decay times.

The G band connected to the semiconducting structure of PbI_2 displays a decay time of the order of ten nanoseconds, while the I band, similarly to the A_x band observed in a Pb^{2+} doped KI crystal, reveals a much longer decay time of the order of micro-seconds. In other words, this result suggests that, in the intercalated PbI_2, the basic semiconducting properties of this material are much changed.

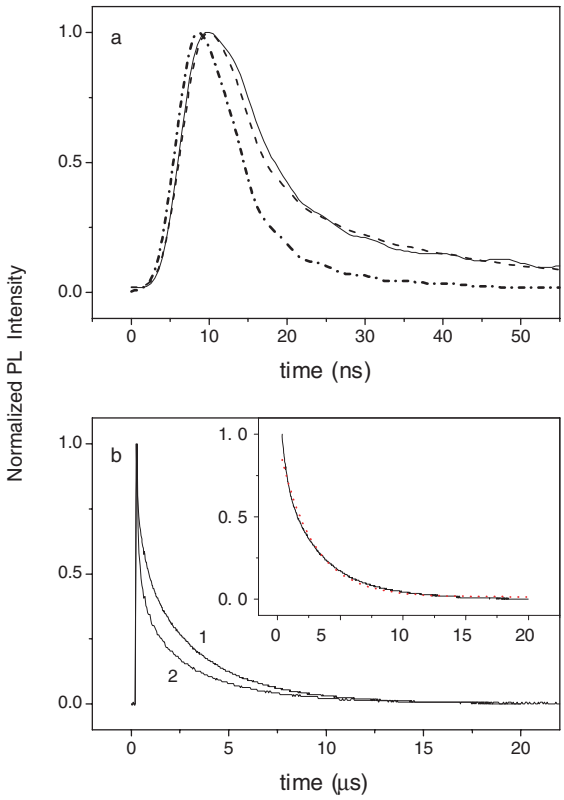

Figure 8. The photoluminescence decay curves at 77 K measured under N_2 laser excitation (337 nm) on the maximum of the G (600 nm) band of PbI_2 crystalline powder (a) and the band I (550 nm) that appears in the intercalated PbI_2, (b). In (a), the dotted and dashed curves show the N_2 laser excitation pulse and the fit using a decay time of 25 ns, respectively. In (b), the curves 1 and 2 show the decay of the I (550 nm) luminescence band of $KPbI_3$ particles and ammonia intercalated PbI_2 samples, respectively. The inset shows the fit (dashed line) using a decay time of 2.6 μs. In both cases, the fit was of single-exponential type.

4. Conclusions

Through correlated studies of scanning electron microscopy, Raman spectroscopy and low-temperature photoluminescence, we have demonstrated that, through the reaction between $Pb(NO_3)_2$ and KI carried out in different liquid media such as water, ethanol, and acetonitrile, platelets and rods of micrometric and nanometric size are formed. By changing the stoichiometry of the synthesis reaction, the yields of platelets and rods can be modified. Platelets are found to be particles of PbI_2 characterized by the same Raman and photoluminescence spectra as the samples prepared from a PbI_2 single crystal grown from the melt. Rods are also obtained by cooling a boiling saturated aqueous PbI_2 solution containing 0.01% poly (vinyl alcohol) or polyacrylamide to room temperature.

Regardless of the preparation method, the rods can be considered as the typical structure of the intercalated PbI_2, being characterized by a distinctive signature in both the Raman and PL spectra. The Raman spectra reveal an orthorhombic structure that results from the intercalation of PbI_2 layers with different molecular species. By way of compression, the intercalation activates a supplementary vibrational mode, associated with the LA phonon, which is observed as a strong Raman band at 30 cm^{-1}.

Due to compression produced by the penetration of foreign molecular species between the iodine layers, the common electronic level formed by the contribution of the 6s and 5p states of Pb^{2+} and I^- ions, which is located at the top of the valence band of the PbI_2 crystal, undergoes a deformation by which the share of the 5p states of I^- ions is reduced. Finally, the PL process into intercalated PbI_2 acquires all the characteristics of luminescence due to an intra-ion transition. Such PL is clearly observed when the Pb^{2+} ions are dissolved in an alkali halide crystal. This transformation is evidenced by a strong emission band at 2.23 eV (about 550 nm) that appears under excitation at higher energy (340 nm; 3.6 eV). This band, investigated using its luminescence decay kinetics, reveals a decay time of the order of a microsecond. This result was considered to be the most convincing evidence to support the idea that, in the intercalated PbI_2, the basic semiconducting properties of the PbI_2 crystal are greatly altered.

References

[1] Jacobson A J 1992 Intercalation reaction of layered compounds *Solid State Chemistry Compounds* ed A K Cheetham and P Day (Oxford: Clarendon) p 182
[2] Lerf A 2000 Intercalation compounds in layered host lattices: supramolecular chemistry in nanodimensions *Handbook of Nanostructured Materials and Nanotechnology* vol 5, ed H S Nalwa (New York: Academic) p 5
[3] Al-Jishi R, Coleman C C, Treece S and Goldwhite H 1989 *Phys. Rev.* B **39** 4862–5
[4] Yu-Hallada L C and Francis A H 1990 *J. Phys. Chem.* **94** 7518–23
[5] Mehrotra V, Lomardo S, Thompson M O and Giannelis E P 1991 *Phys. Rev.* B **44** 5786–90
[6] Warren R F and Liang W Y 1993 *J. Phys.: Condens. Matter* **5** 6407–18
[7] Gurina G I and Savchenco K V 1995 *J. Photochem. Photobiol.* A **86** 81–4
[8] Coleman C C, Magness B, Melo P, Goldwhite H, Tikkanen W, Tham Q, Pham K, Jacubinas R, Kaner R B and Treece R E 1996 *J. Phys. Chem. Solids* **57** 1153–8
[9] Schaeffer R W and Ardelean M 2001 *Powder Diffr.* **16** 16–9
[10] Tubbs M R 1972 *Phys. Status Solidi* b **49** 11–50
[11] Makino T, Gu P, Watanabe M and Hayashi T 1995 *Solid State Commun.* **93** 983–7
[12] Makino T, Watanabe M and Hayashi T 1998 *J. Lumin.* **76/77** 451–4
[13] Mino H, Kawai T, Akai I and Karasawa T 1998 *J. Lumin.* **76/77** 109–12
[14] Mino H, Yamamoto M, Kawai T, Akai I and Karasawa T 2000 *J. Lumin.* **87–89** 278–80
[15] Saito S and Goto T 1995 *Phys. Rev.* B **52** 5929–34
[16] Streelatha K, Venugopal C, Chaudhary S K and Unikrishnam N V 1999 *Cryst. Res. Technol.* **34** 897–900
[17] Idrish M M 2002 *Opt. Mater.* **20** 279–82
[18] Fujisawa J and Ishihara T 2004 *Phys. Rev.* B **70** 113203–7
[19] Ahuja R, Arwin H, Ferreira da Silva A, Persson C, Osorio-Guillen J M, Souza de Almeida J, Moyses Araujo C, Veje E, Veissid N, An C Y, Pepe I and Johansson B 2002 *J. Appl. Phys.* **92** 7219–24
[20] Sandroff C J, Hwang D M and Chung W M 1986 *Phys. Rev.* B **33** 5953–5
[21] Baibarac M, Preda N, Mihut L, Baltog I, Lefrant S and Mevellec J Y 2004 *J. Phys.: Condens. Matter* **16** 2345–56
[22] Calistru D M, Mihut L, Lefrant S and Baltog I 1997 *J. Appl. Phys.* **82** 5391–5
[23] Baltog I, Lefrant S, Mihut L and Mondescu R 1993 *Phys. Status Solidi* b **176** 247–54
[24] Minagawa T 1979 *J. Appl. Crystallogr.* **12** 57–9
[25] Zallen R and Slade M L 1975 *Solid State Commun.* **17** 1561–6
[26] Sears W M, Klein K L and Morrison J A 1979 *Phys. Rev.* B **19** 2305–14
[27] Baltog I, Calistru D, Dimofte C, Mihut L, Mondescu R and Pavelescu G 1992 *Phys. Status Solidi* a **128** 243–52
[28] Baltog I, Lefrant S, Mihut L and Mondescu R 1995 *J. Lumin.* **63** 309–16
[29] Lifshitz E, Yassen M, Bykov L and Dag I 1996 *J. Lumin.* **70** 421–34
[30] Lifshitz E, Bykov L, Yassen M and Chen-Esterlit Z 1997 *Chem. Phys. Lett.* **273** 381–8
[31] Benes L, Melanova K, Zima V, Kalousova J and Votinsky J 1998 *J. Inclusion Phenom. Mol. Recognit. Chem.* **31** 275–86
[32] Marculescu L and Frunza S 1977 *Rev. Roum. Phys.* **22** 813–20
[33] Baltog I, Marculescu L, Mihut L, Frunza S and Ghita C 1980 *Phys. Status Solidi* a **61** 573–8
[34] Baltog I and Mihut L 1984 *Phys. Status Solidi* b **124** 307–13